ACS OMEGA

http://pubs.acs.org/journal/acsodf

Article

Biofabrication of Gold Nanoparticles Using *Capsicum annuum* Extract and Its Antiquorum Sensing and Antibiofilm Activity against Bacterial Pathogens

Faizan Abul Qais,* Iqbal Ahmad, Mohammad Altaf, and Saad H. Alotaibi

Cite This: *ACS Omega* 2021, 6, 16670−16682

Read Online

ACCESS | Metrics & More | Article Recommendations | Supporting Information

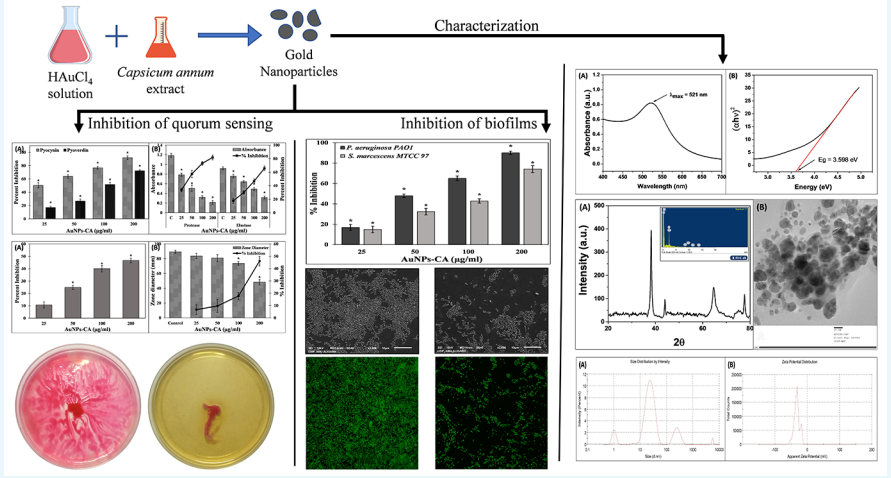

ABSTRACT: The intensive use of antimicrobial agents has led to the emergence of multidrug resistance (MDR) among microbial pathogens. Such microbial (MDR) infections become more problematic in chronic diseases in which the efficacy of chemotherapeutic agents is highly reduced. To combat the problem of drug resistance, inhibition of bacterial quorum sensing (QS) and biofilms are considered as promising strategies in the development of anti-infective agents. In this study, gold nanoparticles (AuNPs-CA) were biofabricated using *Capsicum annuum* aqueous extract and characterized. The AuNPs-CA were tested against the QS-controlled virulence factors and biofilms of *Pseudomonas aeruginosa* PAO1 and *Serratia marcescens* MTCC 97. AuNPs-CA were found to be crystalline in nature with average particle size 19.97 nm. QS-mediated virulent traits of *P. aeruginosa* PAO1 such as pyocyanin, pyoverdin, exoprotease activity, elastase activity, rhamnolipids production, and swimming motility were reduced by 91.94, 72.16, 81.82, 65.72, 46.66, and 46.09%, respectively. Similarly, dose-dependent inhibition of virulence factors of *S. marcescens* MTCC 97 was recorded by the treatment of AuNPs-CA. The biofilm development and exopolysaccharide (EPS) production also decreased significantly. Microscopic analysis revealed that the adherence and colonization of the bacteria on solid support were reduced to a remarkable extent. The findings indicate the possibility of application of green synthesized gold nanoparticles in the management of bacterial infection after careful in vivo investigation.

INTRODUCTION

Owing to the contribution of infectious diseases in global mortality and morbidity after cancer and cardiovascular diseases, infectious diseases are now considered a serious threat to human health and the environment.[1] The intensive and unprescribed use of antimicrobials is the key factor leading to the emergence of multidrug-resistant (MDR) and extensively resistant (XDR) microorganisms. These drug-resistant microbes further worsen the treatment of infectious diseases by making the antibiotics therapeutically ineffective.[2,3] The spread of antimicrobial resistance (AMR) among bacteria has increased enormously and reached an alarming situation. According to a WHO (2019) report, approximately 700 000 people die annually due to infections caused by drug-resistant microbes. AMR is expected to become the major cause of global mortality by 2050, even surpassing cancer, if no action is taken.[4,5] Moreover, the Centers for Disease Control and

Received: May 1, 2021
Accepted: June 4, 2021
Published: June 16, 2021

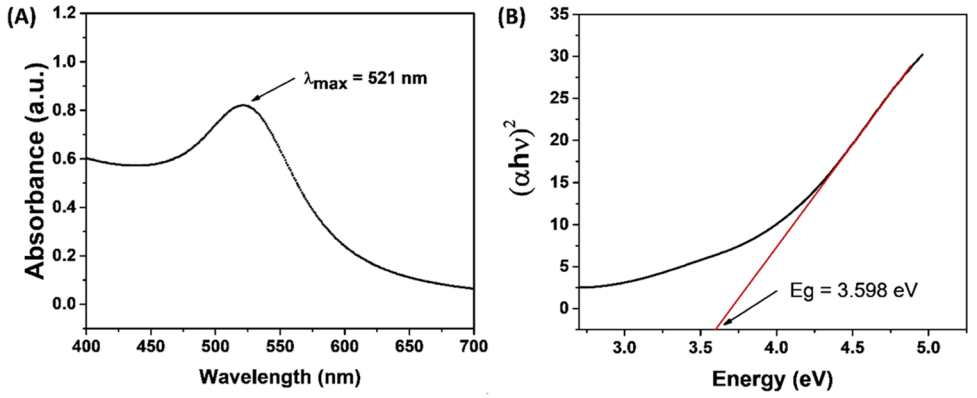

Figure 1. (A) UV−visible absorption spectrum of AuNPs-CA synthesized using *C. annuum* aqueous extract. (B) Band-gap energy in eV of the AuNPs-CA calculated using the Tauc plot.

Prevention (CDC) has documented that each year more than 2 million people become ill due to antibiotic-resistant infections in the United States, which causes roughly 23 000 deaths.[6] Global AMR dissemination and lack of discovery of new antibiotics are the major problems associated with the treatment of infectious diseases. The global AMR threat has triggered urgent calls from international and national agencies to tackle the problem at various stages through integrated approaches by developing new strategies to combat AMR. Inhibition of bacterial communication systems and biofilms of pathogenic bacteria in the development of anti-infective agents are considered as promising strategies.[7,8] These anti-infective agents selectively target microbial virulence without affecting their growth, minimizing the risk of development of drug resistance.[9]

Quorum sensing (QS) is a microbial communication mechanism in which microbes communicate through the biosynthesis and diffusion of signaling molecules (auto-inducers) to control an array of physiological functions. Through QS, microbes coordinate their behavior and regulate the expression of a certain set of genes in a population-dependent manner.[10] QS is known to be involved in the secretion of virulence factors and the expression of antibiotic-resistant genes.[11,12] Earlier, it was thought that microbes grow in the planktonic mode; however, it was found that the majority of the microbes grow in colonies or communities called biofilms.[13] Bacteria reside in self-secreted extrapolymeric substances; these extrapolymeric substances include exopolysaccharides (EPS), proteins, eDNA, etc.[14]

Recent advancement in nanotechnology has received considerable attention in many scientific domains including biomedical science, materials science, medicine, engineering, etc.[15] This has also created new hope in the development of novel antibacterial and anti-infective agents. Typically, nanoparticles are materials with size less than 100 nm. Metal nanoparticles are considered a good choice for biomedical applications such as diagnostics, photothermal therapy, electrical and optical sensing, etc.[16] A large number of metal nanoparticles such as gold, silver, titanium, iron, zinc, etc. have been documented to exhibit antibacterial properties.[17] Moreover, certain nanoparticles have also proved to be potent inhibitors of bacterial biofilms.[18] Owing to such excellent properties of nanoparticles, continuous efforts are being made for the development of inhibitors of biofilms and virulence.

The chemical procedure for metal nanoparticle synthesis is more prevalent. Chemicals synthesis uses certain chemicals as reducing agents to form metal nanoparticles, and these chemicals or their byproducts pose a serious threat to the environment.[19] However, the green route of metal nanoparticle synthesis has advantages over chemical synthesis owing to the use of natural products and being eco-friendly in nature.[20] Moreover, the biodegradable nature of natural products makes it further beneficial and a commonly used material for nanoparticle synthesis. On the contrary, there are some drawbacks associated with the green route of metal nanoparticle synthesis. The major limitation is that the phytochemical profile of natural products changes with climatic and seasonal variation, and these variations greatly influence the specificity and reproducibility in the synthesis of nanoparticles with precise attributes.[21] Moreover, the over-exploitation of natural resources may also result in ecological imbalances.

In this study, gold nanoparticles were prepared using the aqueous extract of *Capsicum annuum*. The major reason for selection of *C. annuum* for gold nanoparticle synthesis is that the extract of this plant has been reported to exhibit antibiofilm activity against *Klebsiella pneumoniae*, *Pseudomonas aeruginosa*, and *Escherichia coli*.[22] The active phytoconstituents of *Capsicum frutescens* and *C. annuum* extracts have been found to mitigate the QS-controlled virulent phenotypes of bacteria.[23] Moreover, gold nanoparticles have also been found to exhibit anti-QS potential.[24] Therefore, it is expected that gold nanoparticles and phytoconstituents of *C. annuum* will impart enhanced efficacy against the biofilms and QS of pathogenic bacteria. The nanoparticles were characterized in detail. The antivirulence and antibiofilm activities of the gold nanoparticles were tested against Gram-negative bacteria viz. *P. aeruginosa* PAO1 and *Serratia marcescens* MTCC 97. The effect of biofabricated nanoparticles was assessed on the architecture of the biofilm using an array of microscopic tools such as light, confocal microscopy, and electron microscopy.

RESULTS AND DISCUSSION

Characterization of AuNPs-CA. The preliminary characterization of AuNPs-CA was carried by monitoring the UV−vis absorption spectrum. UV−vis absorption spectroscopy is a routinely used technique for the characterization of metallic nanoparticles because of the surface plasmon resonance (SPR) phenomenon. SPR is a collective excitation of electrons in the conduction band around the nanoparticle surface. The color of the $HAuCl_4$ solution changed from transparent to light or ruby red, indicating the formation of gold nanoparticles (AuNPs-

https://doi.org/10.1021/acsomega.1c02297
ACS Omega 2021, 6, 16670−16682

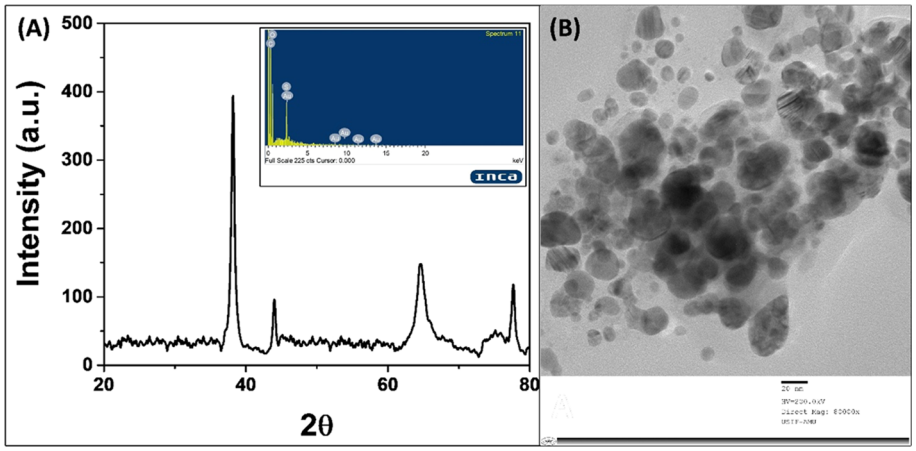

Figure 2. (A) X-ray diffraction pattern of biosynthesized AuNPs-CA using *C. annuum* aqueous extract. Peaks are located at 38.183, 43.990, 64.550, and 77.670°. Energy-dispersive X-ray analysis (EDAX) spectrum of AuNPs-CA (inset). (B) Transmission electron micrograph (TEM) of AuNPs-CA at 80 000× magnification.

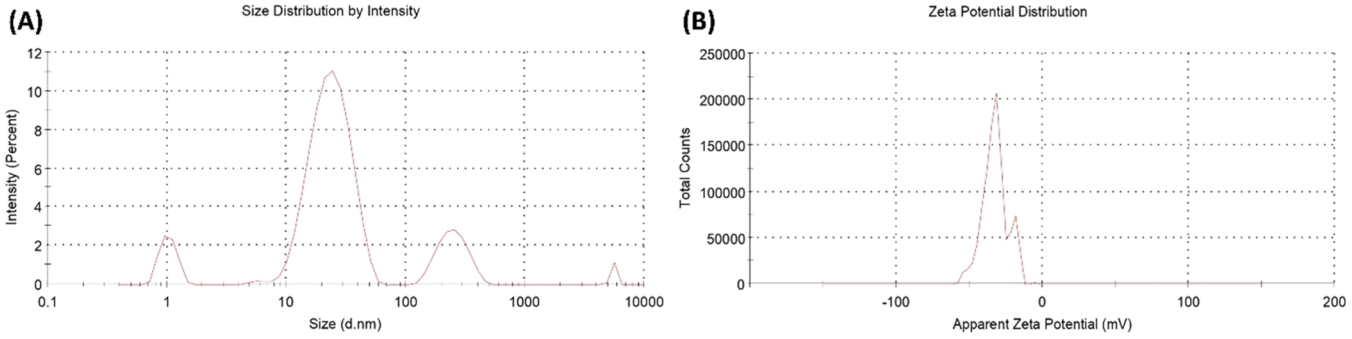

Figure 3. (A) Dynamic light-scattering (DLS) pattern of biosynthesized AuNPs-CA using *C. annuum* aqueous extract. (B) ζ-Potential of biosynthesized AuNPs-CA using *C. annuum* aqueous extract.

CA).[25] The visible red color is due to the reduction of Au^{+3} to Au^0.[2424] The UV−vis absorption spectrum of AuNPs-CA is shown in Figure 1A. The nanoparticles exhibited an absorption peak at 521 nm, which is attributed to the SPR of the gold nanoparticles. This finding is in agreement with an earlier report where gold nanoparticles synthesized using the marine plant, *Padina tetrastromatica*, exhibited SPR at 526 nm.[25] The synthesis of gold nanoparticles using pulp extract of *C. annuum* has been documented in the literature.[26] The nanoparticles were triangular and hexagonal in shape, and some spherical particles were also observed when synthesized at different pH, temperature, and $HAuCl_4$ concentrations. The compounds present in the extract of *C. annuum* are attributed to the reduction of Au^{+3} and synthesis of AuNPs-CA. The band gap was found to be 3.598 eV (Figure 1B), which is consistent with an earlier report.[27]

The X-ray diffraction (XRD) analysis was carried out to obtain the crystallinity and lattice parameters of green synthesized AuNPs-CA (Figure 2A). The XRD pattern of AuNPs-CA exhibited four intense peaks at 2θ values 38.183, 43.990, 64.550, and 77.670°, which correspond to Bragg's reflections of gold nanocrystals.[28] The Debye−Scherrer equation (eq 1) was used to calculate the average crystalline size of AuNPs-CA[29]

$$D_p = \frac{0.9\lambda}{\beta \cos\theta} \quad (1)$$

where D_p is the average crystalline size, λ is the wavelength of Cu Kα (1.54060 Å), θ is the Bragg angle, and β is the full width at half-maximum (FWHM). The average crystalline size of the AuNPs-CA calculated using the Debye−Scherrer formula was found to be 20.80 nm.

The shape and size distribution of AuNPs-CA was analyzed using transmission electron microscopy (TEM). The TEM image of AuNPs-CA is shown in Figure 2B. The shape of AuNPs-CA was observed as spheroidal with some anisotropies. The particles ranged from nearly 7 to 36 nm. The average particle size using TEM was found to be 19.97 nm. The EDAX analysis confirmed that gold was present in AuNPs-CA (Figure 2A inset).

The particle size was further validated using DLS. The particle size distribution analysis by DLS was found to be 26.34 nm (Figure 3A). This is in close agreement with the TEM data. The colloidal solutions exhibiting ζ-potentials ranging from −40.0 to +40.0 mV are generally considered stable. The ζ-potential of AuNPs-CA was found to be −35.2 ± 6.49 mV (Figure 3B), indicating the stable nature of synthesized AuNPs-CA.

Determination of Subinhibitory Concentrations. Before testing the antibiofilm and anti-QS activities of AuNPs-CA, subinhibitory concentrations (sub-MIC) were determined. The test bacteria were cultured in the presence of varying concentrations (62.5, 125, 250, 500, and 1000 μg/mL) of AuNPs-CA to determine the bacterial viability. The presence of 250 μg/mL AuNPs-CA did not alter the bacterial

https://doi.org/10.1021/acsomega.1c02297
ACS Omega 2021, 6, 16670−16682

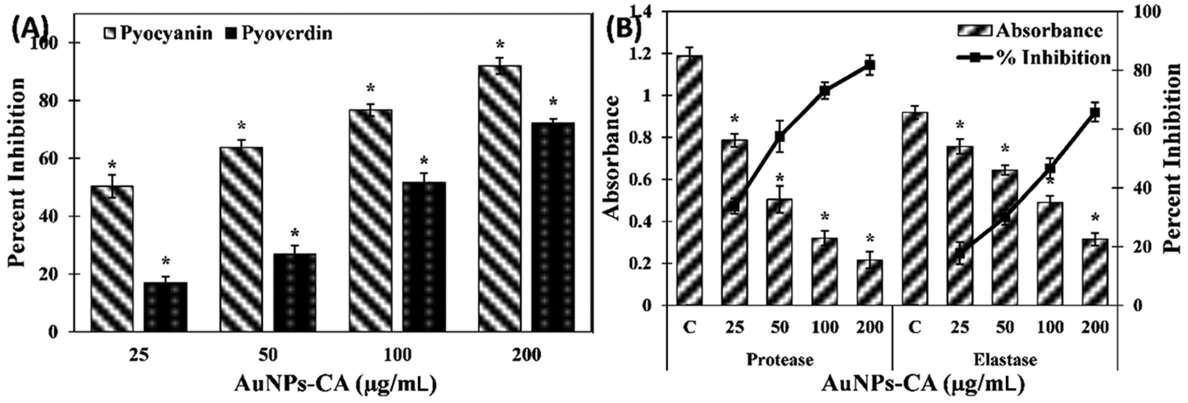

Figure 4. (A) Effect of AuNPs-CA on the pyocyanin and pyoverdin production in *P. aeruginosa* PAO1. (B) Effect of AuNPs-CA on the exoprotease and elastase activity in *P. aeruginosa* PAO1. The data is presented as average ± standard deviation (SD) of three replicates. * indicates *p*-values less than 0.05 with respect to the control.

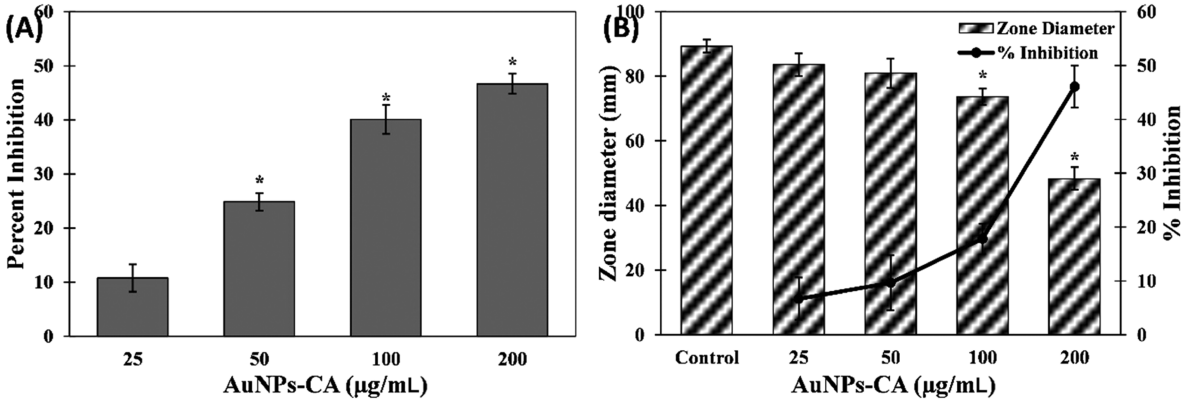

Figure 5. (A) Effect of AuNPs-CA on rhamnolipid production in *P. aeruginosa* PAO1. (B) Effect of AuNPs-CA on the swimming motility of *P. aeruginosa* PAO1. The data is presented as average ± SD of three replicates. * indicates *p*-values less than 0.05 with respect to the control.

growth. Furthermore, the CFU of the bacteria was determined in the absence and presence of 200 μg/mL AuNPs-CA (Figure S1). At this concentration, insignificant (*p*-value > 0.05) differences in $\log_{10}$ CFU were recorded. Therefore, we have selected 200 μg/mL and lower concentrations (100, 50, and 25 μg/mL) to assess the virulence factors and biofilms.

Inhibition of Quorum-Sensing-Controlled Virulence Factors of *P. aeruginosa* PAO1. The effect of AuNPs-CA was examined against six different virulence factors of *P. aeruginosa* PAO1 that are governed by QS. For comparative assessment, all tested virulence factors of *P. aeruginosa* PAO1 and *S. marcescens* MTCC 97 are presented in Table S1.

Many virulent strains of *P. aeruginosa* secrete a blue-green pigment called pyocyanin. The production of pyocyanin is controlled by bacterial cell-to-cell communication, i.e., QS.[30] In the untreated control group of *P. aeruginosa* PAO1, the concentration of pyocyanin was found to be 5.93 ± 0.39 μg/mL, which decreased dose-dependently by treatment of AuNPs-CA, as shown in Figure 4A. The presence of 25, 50, and 100 μg/mL AuNPs-CA in the culture media decreased the pyocyanin production by 50.28 ± 3.98, 63.75 ± 2.60, and 76.75 ± 2.08%, respectively. At the highest tested concentration (200 μg/mL), more than 90% inhibition of pyocyanin production was recorded. This result is in agreement with previous findings in which green synthesized gold nanoparticles inhibited pyocyanin production in *P. aeruginosa* by >90%.[24] Pyocyanin is a known virulent trait of *P. aeruginosa* that contributes to pathogenicity by interfering with cellular functions of the host system.[31] Pyocyanin and its precursor have been reported to alter the expression of numerous immune modulatory proteins in patients with cystic fibrosis. The secretion of pyocyanin in cystic fibrosis subjects also hinders the normal beating of respiratory cilia in human.[32] Moreover, the establishment of biofilms is supported by pyocyanin and the pigment also causes suppression of the host immune system by inducing apoptosis in human neutrophils.[33]

Another pigment produced by *P. aeruginosa* is pyoverdin. This pigment is fluorescent in nature and secreted by many virulent strains of *P. aeruginosa*.[34] Treatment with varying concentrations of AuNPs-CA resulted in concentration-dependent inhibition of pyoverdin production (Figure 4A). The addition of 25, 50, and 100 μg/mL AuNPs-CA decreased the pyoverdin level by 16.98 ± 2.10, 26.77 ± 3.07, and 51.59 ± 3.19% in the culture supernatant, respectively. The presence of the highest tested concentration (200 μg/mL) inhibited the pyoverdin secretion by 72.16 ± 1.53%. Like pyocyanin, pyoverdin also confers overall virulence to *P. aeruginosa*. The presence of pyoverdin cleaves/detaches the iron from the transferrin protein, which causes deficiency of iron in tissues of the host.[35] Moreover, a study has found that pyoverdin also assists in the establishment of *P. aeruginosa* infection in cystic fibrosis patients.[34] Therefore, the inhibition of these pigments depicts the protective effect of AuNPs-CA by decreasing the virulence of *P. aeruginosa* PAO1.

https://doi.org/10.1021/acsomega.1c02297
ACS Omega 2021, 6, 16670−16682

Table 1. Effect of AuNPs-CA on Inhibition of Virulence Factors in *S. marcescens* MTCC 97[a]

AuNPs-CA concentration	virulence factor production			
	prodigiosin[c]	protease activity[d]	cell surface hydrophobicity[e]	swarming motility[f]
control	1.241 ± 0.039	0.736 ± 0.021	64.83 ± 4.02	89.66 ± 0.57
25 μg/mL	0.930 ± 0.029[bI] (25.07)	0.664 ± 0.016 (09.69)	44.83 ± 3.97[bI]	88.33 ± 1.52 (01.48)
50 μg/mL	0.748 ± 0.036[bI] (39.73)	0.546 ± 0.020[bI] (25.81)	35.53 ± 2.21[bI]	72.66 ± 4.50[bI] (18.95)
100 μg/mL	0.452 ± 0.079[bI] (63.59)	0.430 ± 0.021[bI] (41.48)	21.16 ± 1.95[bI]	63.33 ± 5.03[bI] (29.36)
200 μg/mL	0.268 ± 0.011[bI] (78.41)	0.311 ± 0.014[bI] (57.65)	12.03 ± 2.99[bI]	24.33 ± 7.37[bI] (72.86)

[a]The data are presented as average ± SD of three replicates. For analysis of statistical significance, the *t*-test was performed. [bI]ndicates *p*-values less than 0.05 with respect to the control. Values in parenthesis are the percent inhibition. [c]Prodigiosin pigment is expressed as the absorbance at 534 nm. [d]Protease activity is expressed as the absorbance at 400 nm. [e]Cell surface hydrophobicity (CSH) is expressed as percentage. [f]Swimming motility is expressed as swarm diameter in mm.

Exoproteases and elastases are the major enzymes secreted by virulent strains of pathogenic or opportunistic bacteria that suppress the host immune response and cause degradation of host tissues.[36] The effect of AuNPs-CA on the production of these two enzymes was assessed, and the results are presented in Figure 4B. The presence of 25, 50, 100, and 200 μg/mL AuNPs-CA resulted in 33.77 ± 2.59, 57.47 ± 5.41, 73.04 ± 2.87, and 81.82 ± 3.36% decreases in the exoprotease activity in the supernatant of *P. aeruginosa* PAO1, respectively. Similarly, treatment with 25, 50, 100, and 200 μg/mL AuNPs-CA inhibited the elastase activity by 17.71 ± 3.75, 29.96 ± 2.53, 46.66 ± 3.36, and 65.72 ± 3.25%, respectively. One of the mechanisms of bacterial invasion in host tissues is cleaving the cell proteins by proteases and weakening the immune response.[37] The establishment of biofilms is also modulated by the synthesis of las proteins whose synthesis is governed by QS in *P. aeruginosa*.[38] Previously, gold nanoparticles synthesized using fucoidan have been reported to inhibit the production of proteases.[39] Other metal nanoparticles such as silver nanoparticles have been documented to inhibit the exoprotease activity of *P. aeruginosa* PAO1. The study also found that silver nanoparticles downregulated the *lasB* gene expression and ultimately reduced the elastinolytic activity of *P. aeruginosa*.[40] The inhibition of elastinolytic and proteolytic activity shows the modulatory effect of AuNPs-CA on modulation of *lasI-lasR* QS of *P. aeruginosa*.

P. aeruginosa secretes surfactants called rhamnolipids, which help in the adherence of bacterial cells to solid support as well as in the maintenance of the architecture of biofilms.[41] AuNPs-CA exerted a dose-dependent inhibitory effect on the production of rhamnolipid in supernatants of *P. aeruginosa* PAO1 (Figure 5A). The addition of 25, 50, 100, and 200 μg/mL AuNPs-CA in culture media decreased rhamnolipid production by 10.77 ± 2.51, 24.85 ± 1.58, 40.08 ± 2.71, and 46.66 ± 1.85%, respectively. Rhamnolipids also help in the motility of *P. aeruginosa* on solid surfaces,[42] and the findings of this study show the protective effect of AuNPs-CA. The motility of *P. aeruginosa* results in the spread of the infection in the host, and this virulence factor is also controlled by QS.[43] The zone of the swimming diameter of *P. aeruginosa* PAO1 in the absence and presence of AuNPs-CA on soft agar plates is shown in Figure 5B. In control plates, *P. aeruginosa* PAO1 swam to the entire plate. At lower concentrations (25 and 50 μg/mL) of AuNPs-CA, an insignificant (p-value > 0.05) reduction in swimming of *P. aeruginosa* PAO1 was found. However, at higher tested concentrations (100 and 200 μg/mL), the motility was reduced by 17.84 ± 2.82 and 46.09 ± 3.94%, respectively. This finding is in agreement with earlier reports where gold nanoparticles synthesized using fucoidan decreased the swarming, swimming, and twitching motility.[39]

Nanoparticles have been found to be potent inhibitors of QS by altering the bacterial cell-to-cell communication. However, the exact underlying mechanism of QS inhibition by nanoparticles is not fully understood. Studies have proposed two possible mechanisms, which are the dampening of synthesis of signal molecules and the prevention of formation of a complex with receptor proteins.[44] A study conducted on silver nanoparticles has found that the nanoparticles effectively blocked the active sites to inhibit the expression of QS-controlled genes by blocking regulatory proteins of transcription. This resulted in inactivation of the LasR or RhlR system.[45] These studies led us to explain the possible mechanism of anti-QS activity of AuNPs-CA, which may be the inhibition of signal molecule synthesis, prevention of binding of signal molecules to receptor proteins, and/or blocking the active site of QS regulatory proteins.

Inhibition of Virulence Factors of *S. marcescens* MTCC 97. To check the broad-spectrum anti-QS activity, the effect of AuNPs-CA was also tested against virulence factors of *S. marcescens* MTCC 97. *S. marcescens* secretes a pink-red pigment, which is controlled by QS. There are four different acylhomoserine lactone (AHL) molecules that govern many virulent traits of *S. marcescens* such as prodigiosin production, biofilm formation, motility, and carbapenem resistance.[46] It is evident from the data presented in Table 1 that increasing concentrations of AuNPs-CA subsequently inhibited the production of prodigiosin in *S. marcescens* MTCC 97. The presence of 25, 50, 100, and 200 μg/mL AuNPs-CA inhibited prodigiosin production by 25.07 ± 2.34, 39.73 ± 2.95, 63.59 ± 6.36, and 78.41 ± 0.94%, respectively. A study documented that there may be some common regulatory link in prodigiosin biosynthesis, hemagglutination, and flagellar variation in *S. marcescens*.[47] Bacterial pigments, such as prodigiosin, modulate the immune responses and induce cytotoxicity in host cells.[31,48] Moreover, pigments produced by bacteria are also essential to their survival and contribute to their pathogenicity.[48] Earlier, silver nanoparticles synthesized using *Piper betle* aqueous extract had been reported to inhibit prodigiosin production in *S. marcescens*.[49] A similar effect on the azocasein degrading exoprotease activity in *S. marcescens* MTCC 97 was also recorded in the presence of AuNPs-CA (Table 1). Treatment with 25, 50, 100, and 200 μg/mL AuNPs-CA resulted in 9.69 ± 2.28, 25.81 ± 2.72, 41.48 ± 2.93, and 57.653 ± 1.97% decreases in proteolytic activity in cell-free supernatants, respectively. The secretion of proteolytic enzymes is responsible for inducing immune response and establishment of infection in the host.[50]

https://doi.org/10.1021/acsomega.1c02297
ACS Omega 2021, 6, 16670−16682

The cell surface hydrophobicity (CSH) of *S. marcescens* plays a key role in adherence to solid surfaces and development of biofilms.[51] AuNPs-CA successfully inhibited the CSH of *S. marcescens* MTCC 97 (Table 1). In the untreated control group *S. marcescens* MTCC 97, CSH was found to be 64.83 ± 4.02%. The presence of 25, 50, 100, and 200 μg/mL AuNPs-CA decreased the CSH of *S. marcescens* MTCC 97 to 44.83 ± 3.97, 35.53 ± 2.21, 21.16 ± 1.95, and 12.03 ± 2.99%, respectively. The hydrophobic index of the cell surface of bacteria is important for initial attachment and biofilm formation, and hence targeting CSH is an alternate strategy for the inhibition of biofilms. A similar activity has been reported earlier where silver nanoparticles synthesized using root extract of *Vetiveria zizanioides* inhibited the CSH of *S. marcescens*.[52] The swimming motility is a characteristic feature of some virulent strains of *S. marcescens*, and it plays an important role in certain nosocomial infections such as urinary tract infections (UTIs) associated with catheters.[51] In the absence of AuNPs-CA, *S. marcescens* MTCC 97 swarmed the entire Petri plate with a dark-red-pink pigment production. At the lowest tested concentration (25 μg/mL) of AuNPs-CA, no inhibition in swarming motility was found. However, the presence of 50, 100, and 200 μg/mL AuNPs-CA inhibited the swarming motilities by 18.95 ± 5.01, 29.36 ± 5.59, and 72.86 ± 8.19%, respectively. The motility in *S. marcescens* is assisted by flagella that regulates the initial attachment and plays a key role in biofilm development in UTIs.[53] To the best of our knowledge, this is the first report on the detailed inhibition of QS-controlled virulence factors of *S. marcescens* by green synthesized gold nanoparticles.

For green synthesized gold nanoparticles to be used as anti-infective agents, the particles must not be toxic to the host, i.e., human cells. Upon literature survey, we found varied results for the cytotoxicity of gold nanoparticles on different cell lines. The cytotoxicity of gold nanoparticles depends on many factors such as the method of synthesis, nature of extract used for synthesis, targeted cells (normal or cancer), etc. Some studies have found that gold nanoparticles are toxic to both normal and cancer cell lines.[54,55] However, a review conducted on gold-nanoparticle-induced cell death has found that biosynthesized gold nanoparticles are biocompatible with normal human cells while showing potent cytotoxicity against cancer cells.[56] The cytotoxicity of AuNPs-CA on normal human cells needs to be explored further.

Inhibition of Biofilm Development by AuNPs-CA. The quantitative inhibition of biofilm development was assessed by a standard crystal violet assay in 96-well polystyrene plates. Biofilms have clinical significance where development of biofilms by pathogenic or opportunistic microbes results in successful establishment of infections. AuNPs-CA exhibited a dose-dependent response on biofilm formation of test bacteria, as shown in Figure 6. The presence of 25, 50, and 100 μg/mL AuNPs-CA inhibited the biofilms of *P. aeruginosa* PAO1 by 16.96 ± 3.02, 47.98 ± 1.66, and 65.03%, respectively. Treatment with the highest concentration (200 μg/mL) of AuNPs-CA resulted in more than 90% inhibition of biofilms of *P. aeruginosa* PAO1. Similarly, there were 14.89 ± 3.20, 32.36 ± 3.21, 42.88 ± 2.10, and 74.12 ± 3.45% reductions in biofilm development of *S. marcescens* MTCC 97 in the presence of 25, 50, 100, and 200 μg/mL AuNPs-CA, respectively. In clinical settings, it has become clear that biofilms are more prevalent than it was originally believed.[57] Biofilms are not only found in acute infections but also implicated in a number of chronic

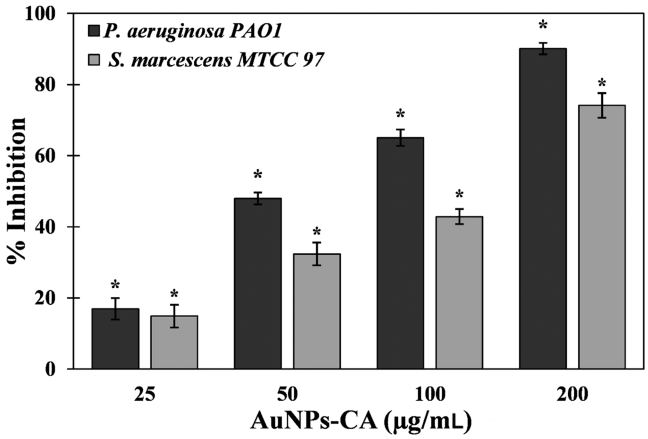

Figure 6. Effect of AuNPs-CA on the development of biofilms of *P. aeruginosa* PAO1 and *S. marcescens* MTCC 97. The data are presented as average ± SD of three replicates. * indicates *p*-values less than 0.05 with respect to the control.

infections such as cystic fibrosis, dental caries, otitis media, periodontal disease, etc.[58] There is also evidence indicating that biofilms hamper the healing of chronic wounds.[59] Once the biofilms are established in persistent infections, there are rare chances of healing only by the immune response.[60] Moreover, the bacteria in persistent infections respond inconsistently to antimicrobial chemotherapeutics.[61] Bacteria coordinate the expression of virulence factors and drug-resistant genes in the biofilm mode of growth. For instance, a study has documented that *P. aeruginosa* growing in the biofilm mode on urinary catheters were found to be 1000-fold more resistant to tobramycin compared to the planktonic growth.[62] Intracellularly synthesized gold nanoparticles using *Laccaria fraternal* have been reported to inhibit biofilms of *P. aeruginosa*. The composition of gold in nanoparticles was nearly 15%, and the particles reduced the biofilms by 93%.[24] It has been documented that change in chemical and physical properties of the nanoparticles may influence the antibacterial activity and bacterial toxicity.[63,64] It is evident from data that AuNPs-CA inhibited the biofilm development of Gram-negative bacterial pathogens to a remarkable extent.

The nanoparticles are known to interact with the extrapolymeric matrix of biofilms. This interaction is mainly governed by their electrostatic forces owing the ζ-potential of nanoparticles and charges on biofilms. The nanoparticles also have the tendency to diffuse in the biofilm matrix.[65] Based on the previous reports, we can say that the possible mechanisms of antibiofilm activity of AuNPs-CA may be mechanical damage to the bacterial cell wall, oxidative stress due to production of ROS, and/or disruption of the protein assembly or functions due to release of metal ions.[66]

Inhibition of Biofilms on Glass Surface. The inhibitory effect of AuNPs-CA on biofilm development on a glass surface was further examined microscopically. The detailed changes in biofilm architecture were studied using light microscopy, confocal microscopy, and scanning electron microscopy (SEM).

Light Microscopy. The bacterial cultures were grown in the absence and presence of AuNPs-CA on glass coverslips in 24-well polystyrene tissue culture plates. The light microscopic images of *P. aeruginosa* PAO1 and *S. marcescens* MTCC 97 biofilms in the absence and presence of AuNPs-CA are shown in Figure 7. The untreated control of both bacteria formed

https://doi.org/10.1021/acsomega.1c02297
ACS Omega 2021, 6, 16670−16682

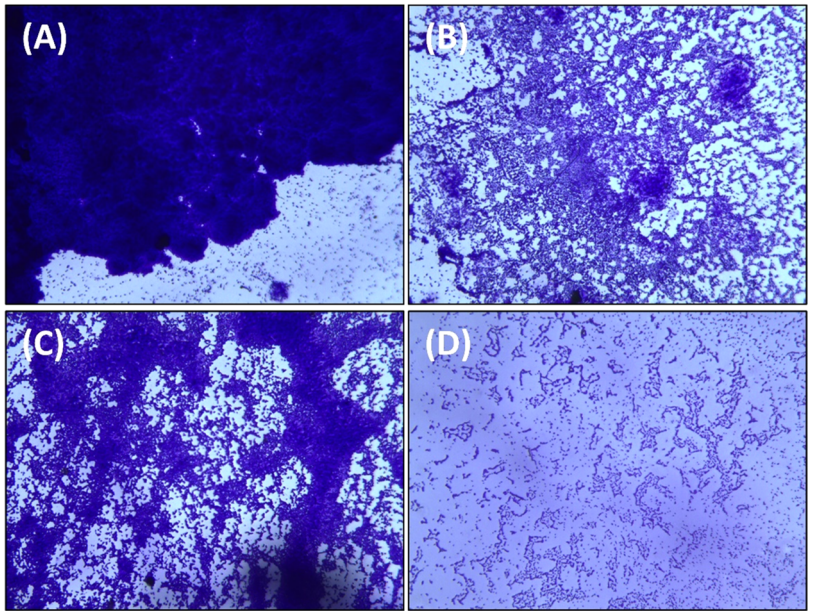

Figure 7. Light microscopic images of the biofilms of *P. aeruginosa* PAO1 and *S. marcescens* MTCC 97 in the absence and presence of AuNPs-CA. (A) Control *P. aeruginosa* PAO1; (B) *P. aeruginosa* PAO1 treated with 200 μg/mL AuNPs-CA; (C) control *S. marcescens* MTCC 97; and (D) *S. marcescens* MTCC 97 treated with 200 μg/mL AuNPs-CA.

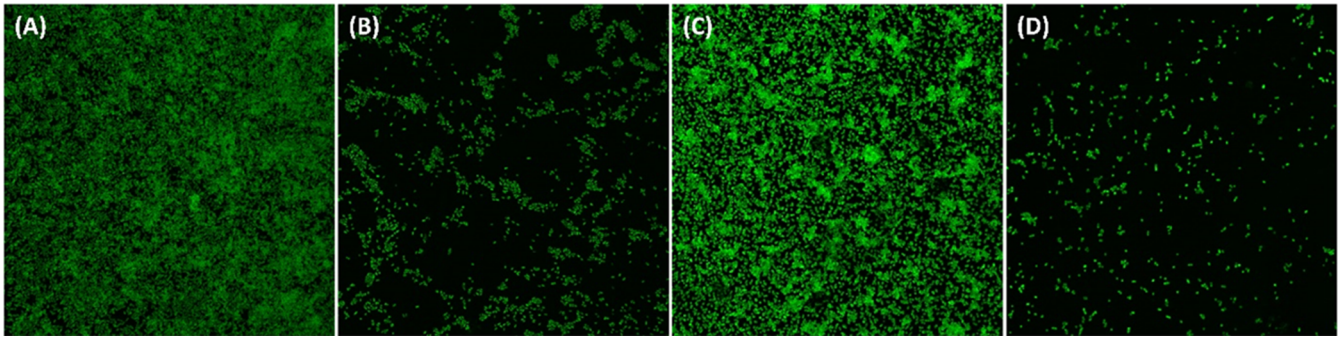

Figure 8. Confocal microscopic images of the biofilms of *P. aeruginosa* PAO1 and *S. marcescens* MTCC 97 in the absence and presence of AuNPs-CA. (A) Control *P. aeruginosa* PAO1; (B) *P. aeruginosa* PAO1 treated with 200 μg/mL AuNPs-CA; (C) control *S. marcescens* MTCC 97; and (D) *S. marcescens* MTCC 97 treated with 200 μg/mL AuNPs-CA.

dense biofilms with a thick layer of cells on the glass surface. Bacteria were heavily colonized on the surface forming a thick cluster of cells. When the cultures were treated with AuNPs-CA, the biofilm-forming ability of both bacteria was remarkably reduced. As evident from the microscopic images, the bacterial colonization decreased and their adherence on the glass surface was greatly reduced. The results are in agreement with a previous finding where gold nanoparticles synthesized using a marine plant, *P. tetrastromatica*, inhibited the biofilm development of *Staphylococcus aureus*.[25]

Confocal Microscopy. For confocal microscopic analysis, the biofilms were stained with acridine orange and visualized using a confocal laser scanning microscope. The confocal microscopic images of *P. aeruginosa* PAO1 and *S. marcescens* MTCC 97 biofilms with and without treatment of AuNPs-CA are presented in Figure 8. As evident from the micrographs, there were dense biofilms on the glass surface of the untreated control of both bacteria. The glass surface was observed to be heavily colonized by bacteria with a thick aggregate of cells in biofilms. Treatment with AuNPs-CA resulted in the reduction of biofilms on glass coverslips. Moreover, cells were seen as scattered in which few cells were capable of colonization. A similar finding has been reported in which the inhibition of biofilms of *P. aeruginosa* by green synthesized gold nanoparticles was shown by fluorescence microscopy.[25]

Scanning Electron Microscopy. A detailed analysis on the effect of AuNPs-CA on the biofilm architecture was performed by electron microscopic analysis. The scanning electron micrographs of *P. aeruginosa* PAO1 and *S. marcescens* MTCC 97 biofilms are depicted in Figure 9. The untreated cells of *P. aeruginosa* PAO1 were seen as a thick cluster of cells with a smooth morphology. The bacterial cells were also enclosed in the polymeric matrix. The presence of AuNPs-CA in culture media extensively decreased the biofilm-forming potential of *P. aeruginosa* PAO1 on the glass surface. The bacterial cells were found to be scattered with a reduced colonization. A similar observation was found for *S. marcescens* MTCC 97 where the untreated control showed an extensive biofilm with a mass of aggregated cells on the glass coverslips. Treatment with AuNPs-CA inhibited the bacterial colonization and, subsequently, the biofilm formation. The SEM analysis showed the inhibition of biofilms of *P. aeruginosa* PAO1 and *S.*

https://doi.org/10.1021/acsomega.1c02297
ACS Omega 2021, 6, 16670−16682

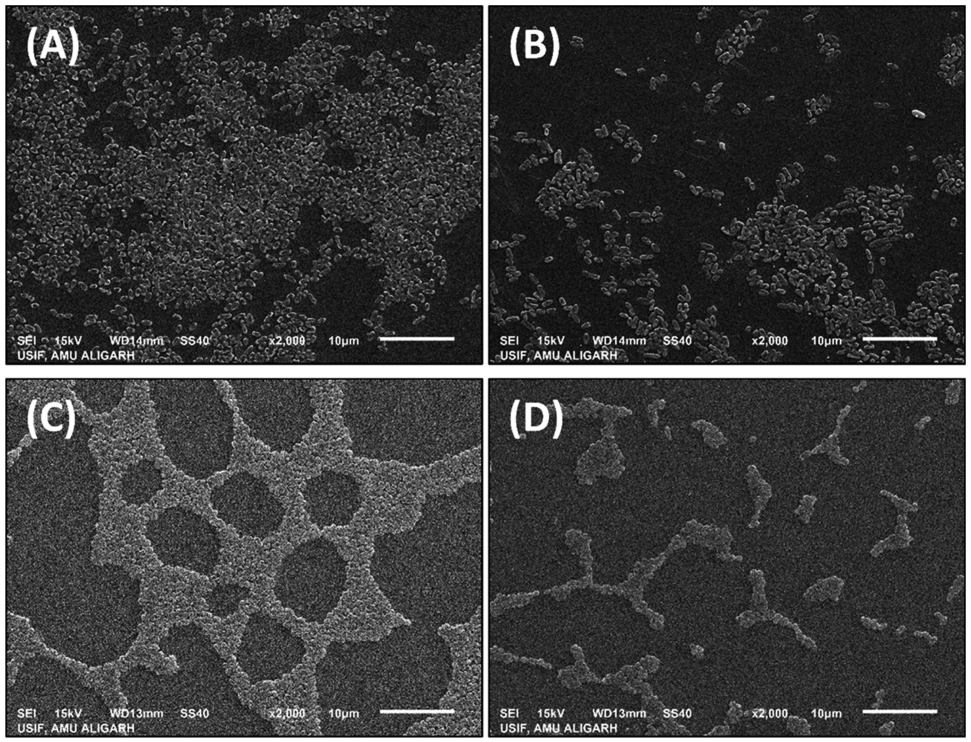

Figure 9. Scanning electron microscopic images of the biofilms of *P. aeruginosa* PAO1 and *S. marcescens* MTCC 97 in the absence and presence of AuNPs-CA. (A) Control *P. aeruginosa* PAO1; (B) *P. aeruginosa* PAO1 treated with 200 μg/mL AuNPs-CA; (C) control *S. marcescens* MTCC 97; and (D) *S. marcescens* MTCC 97 treated with 200 μg/mL AuNPs-CA.

marcescens MTCC 97 with an altered biofilm architecture of the test bacteria.

Electron microscopic analysis gave a visual validation of the biofilm inhibition by AuNPs-CA. A similar finding has been reported previously in which the structural modification of *P. aeruginosa* biofilms was examined using atomic force microscopy. The biofilms were found to be disrupted by the treatment of gold nanoparticles.[67] The matrix of bacterial biofilms contains water channels through which the transport of nutrients occurs. AuNPs-CA might be able to diffuse into the biofilm matrix and reduce the formation of biofilms.

Inhibition of Exopolysaccharide (EPS) Production by AuNPs-CA. Microbes secrete a vast number of large molecules that are collectively termed extracellular polymeric substances or exopolymers. These exopolymers facilitate the adherence of bacteria to solid support, leading to the formation of a complex microbial architecture called biofilms.[68] Among bacterial exopolymers, exopolysaccharides (EPS) constitute the major portion. EPS helps in development of bacterial microcolonies and also aids in the maintenance of the biofilm architecture.[69] EPS confers drug (antimicrobial) resistance and serves as a protective barrier for bacterial cells by restricting the entry of chemotherapeutic agents.[70] Moreover, the elevated secretion of EPS alters the biofilm architecture in such a way that it imparts resistance to antimicrobial agents.[71] Targeting EPS secretion by bacteria is also a novel target for antibacterial drug discovery because of the positive correlation between biofilm formation and EPS secretion.[72] The effect of AuNPs-CA on EPS production in *P. aeruginosa* PAO1 and *S. marcescens* MTCC 97 was assessed, and the results are presented in Figure 10. Treatment with 25, 50, 100, and 200 μg/mL AuNPs-CA resulted in 13.24 ± 2.42, 26.60 ± 4.09, 58.50 ± 2.60, and 84.83 ± 3.88% decreases in EPS secretion of *P. aeruginosa* PAO1,

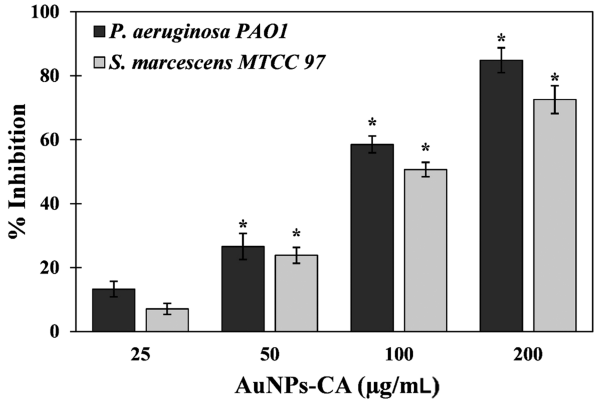

Figure 10. Effect of AuNPs-CA on EPS production in *P. aeruginosa* PAO1 and *S. marcescens* MTCC 97. The data are presented as average ± SD of three replicates. * indicates *p*-values less than 0.05 with respect to the control.

respectively. At the lowest tested concentration (25 μg/mL), insignificant (*p*-value > 0.05) reduction in EPS of *S. marcescens* MTCC 97 was found. However, 23.84 ± 2.48, 50.64 ± 2.24, and 72.51 ± 4.35% inhibition was recorded in the presence of 50, 100, and 200 μg/mL AuNPs-CA, respectively. A similar finding was reported earlier where gold-nanoparticle-synthesized baicalein reduced the EPS production of *P. aeruginosa* PAO1 by more than 80% at 1000 μg/mL.[73] The EPS inhibition by AuNPs-CA supports the biofilm inhibition data and provides a possible mode of antibiofilm activity.

CONCLUSIONS

In this study, gold nanoparticles (AuNPs-CA) were synthesized using *C. annuum* extract. The crystalline nature of

https://doi.org/10.1021/acsomega.1c02297
ACS Omega 2021, 6, 16670−16682

AuNPs-CA was confirmed using XRD analysis, and the average size of nanoparticles was found to be 19.97 nm. QS-controlled virulence factors of *P. aeruginosa* PAO1 and *S. marcescens* MTCC 97 such as pyocyanin, prodigiosin, pyoverdin, exoprotease activity, elastase activity, rhamnolipids production, cell surface hydrophobicity, and motility were remarkably inhibited by AuNPs-CA. Moreover, biofilm formation and EPS production of both test bacteria were decreased by the application of AuNPs-CA. Finally, the microscopic examination of biofilms confirmed that colonization of bacteria on glass coverslips was reduced to a remarkable extent. The findings indicate the potency of gold nanoparticles against bacterial infection, and they may be developed as biofilms and QS inhibitors after careful in vivo investigation.

MATERIALS AND METHODS

Materials and Chemicals. Orcinol and trichloroacetic acid (TCA) were procured from HiMedia Laboratories, India. Elastin−Congo red (ECR) and azocasein were purchased from Sigma Aldrich. All organic solvents were obtained from Thermo Fisher Scientific, India.

Plant Material and Extract Preparation. The fruits of *C. annuum* L. (chili pepper) were obtained from an authorized shop at the local market at Aligarh, UP, India. The plant material was air-dried at room temperature in the shade for 15 days and ground in a mixer grinder to make a fine powder. For the preparation of aqueous extract, 5 gm of plant powder was mixed in 100 mL of double-distilled water and heated at 95 °C for 30 min. The mixture was then left at room temperature for 3 h with intermittent shaking. The suspension was centrifuged and then filtered using a filter paper to obtain the extract. The extract was stored at −20 °C for further use.

Synthesis of Gold Nanoparticles. Stock solution (1 mM) of $HAuCl_4$ was made in double-distilled water. For synthesis of gold nanoparticles, 30 mL of $HAuCl_4$ solution was mixed with 70 mL of plant extract and placed on a magnetic stirrer for 2 h. The color of the reaction mixture turned red/ruby red, indicating the formation of gold nanoparticles.[74] The reaction mixture was centrifuged at 15 000 rpm for 45 min to obtain gold nanoparticles (AuNPs-CA). The nanoparticle pellet was washed twice with double-distilled water to remove the excess of water-soluble phytocompounds or biomolecules. The nanoparticles were dried overnight in an oven at 55 °C and stored at −4 °C in the powdered form. A fresh suspension was made in double-distilled water for experimental usage.

Characterization of AuNPs-CA. The UV-spectroscopic characterization of AuNPs-CA was performed using a UV-2600 spectrophotometer, Shimadzu, Japan. The absorbance spectrum of the AuNPs-CA suspension was recorded from 300 to 700 nm. Double-distilled water was used as the blank.

The band-gap energy of AuNPs-CA was determined using the Tauc relation. As per the Tauc relation, the absorption coefficient for the direct band-gap material was calculated using eq 2

$$\alpha h\nu = A(h\nu - E_g)^m \quad (2)$$

where A is the optical constant, E_g is the band gap, α is the absorption coefficient, and m is the index.[75]

The X-ray diffraction pattern was recorded with an X-ray diffractometer (MiniFlex-II XRD system, Rigaku Corporation, Tokyo, Japan). To record the diffraction pattern, Cu Kα radiation (λ = 1.54060 Å) was used. The 2θ range for XRD analysis was 20−80°. The average particle size of AuNPs-CA was calculated using the Debye−Scherrer formula. The particle size distribution and ζ-potential were obtained using DynaPro-TC-04 dynamic light-scattering (DLS) instrument attached to a ZetaSizer (Malvern, U.K.). The aqueous suspension of AuNPs-CA was used for DLS measurements.

The transmission electron microscopic (TEM) analysis of AuNPs-CA was performed using JOEL-2100, Tokyo, Japan, at the University Sophisticated Instrumentation Facility (USIF), AMU, Aligarh, India. Briefly, 10 μL of an aqueous suspension of AuNPs-CA was placed on a TEM grid and air-dried at room temperature. The grid was used for TEM analysis, and the particle size distribution was obtained by measuring the size of nanoparticles.

To confirm the presence of gold in AuNPs-CA, energy-dispersive X-ray (EDAX) analysis was performed. The fine powder of AuNPs-CA was placed on a microscopic slide for analysis. The analysis was performed using an INCAx-sight EDAX spectrometer (Oxford Instruments).

Bacterial Strains and Culture Conditions. In this study, *P. aeruginosa* PAO1 and *S. marcescens* MTCC were used for the determination of antibiofilm and anti-QS activities. The inocula of the cultures for each experiment were grown in Luria−Bertani medium. For the inoculum, *P. aeruginosa* PAO1 and *S. marcescens* were grown in LB for 4 h and then OD (600 nm) was adjusted to 0.1. A total of 100 μL of adjusted OD was used as the inoculum in 5 mL of broth, which corresponds to ~10^6 CFU/mL. For motility assays, 5 μL of adjusted OD was directly spotted onto the soft agar plates. *P. aeruginosa* PAO1 was grown at 37 °C, while *S. marcescens* MTCC 97 was grown at 30 °C.

Assessment of Virulence Factors of *P. aeruginosa* PAO1. For the assessment of virulence factors of *P. aeruginosa* PAO1, the culture was grown in Luria−Bertani medium (unless stated) in the absence and presence of varying concentrations (25−200 μg/mL) of AuNPs-CA. The cultures were incubated for 18 h at 37 °C in a shaking incubator. Following incubation, the cultures were centrifuged at 8000 rpm for 10 min and the supernatant was collected. All virulence factors were determined in cell-free supernatants unless otherwise stated. For each experiment, fresh cell-free supernatant was used.

For pyocyanin estimation, the bacteria were grown in *Pseudomonas* broth (PB) as this medium increases production of pyocyanin.[76] The bacterial culture was grown in the absence and presence (25−200 μg/mL) of AuNPs-CA at 37 °C for 18 h under the shaking condition. Then, 5 mL of culture from the control and each treatment group was centrifuged to obtain cell-free supernatant. Next, 3 mL of chloroform was added to the cell-free supernatant and mixed by vigorous vortexing to extract the pyocyanin. The aqueous layer was discarded, and the organic layer was again extracted in 1.2 mL of 0.2 N HCl. The absorbance of the aqueous layer was recorded at 520 nm using a UV-2600 spectrophotometer. As a blank, 0.2 N HCl was used.

For pyoverdin assessment, 0.1 mL of the cell-free supernatant was mixed with 0.9 mL of 50 mM Tris-HCl (pH 7.4). The fluorescence intensity of the samples was measured at 460 nm using an RF-5301PC spectrofluorometer (Shimadzu, Japan). The excitation wavelength was 400 nm.[77]

For the assessment of rhamnolipids, 0.3 mL of the cell-free supernatant was added to 0.6 mL of diethyl ether and vortexed for 1 min for proper mixing. The organic phase (diethyl ether)

https://doi.org/10.1021/acsomega.1c02297
ACS Omega 2021, 6, 16670−16682

was taken, and the aqueous phase was discarded. The organic phase was dried in 1.5 mL centrifuge tubes by evaporating the diethyl ether at room temperature. Then, 0.1 mL deionized water was added to each tube followed by addition of 0.9 mL of orcinol solution (0.19% w/v orcinol in 53% H_2SO_4). The reaction mixture was heated for 30 min at 80 °C, and then, samples were cooled at room temperature. The absorbance of each sample was recorded at 421 nm using a UV-2600 spectrophotometer.[78]

The proteolytic activity in the cell-free supernatant of *P. aeruginosa* PAO1 was determined by an azocasein degradation assay. Freshly harvested 0.1 mL of culture supernatant was added to 1.0 mL of 0.3% (w/v) azocasein (prepared in 0.05 M Tris-HCl containing 0.5 mM $CaCl_2$, pH 7.5). The mixture was allowed to react for 4 h at 37 °C with intermittent shaking. The reaction was stopped by the addition of 10% w/v ice-cold trichloroacetic acid (0.5 mL). The mixture was centrifuged at 15 000 rpm for 5 min to settle down insoluble azocasein. The absorbance of the supernatant was recorded at 400 nm using a UV-2600 spectrophotometer earlier.[78]

The elastinolytic activity in the cell-free supernatant of *P. aeruginosa* PAO1 was determined by the standard Elastin−Congo red (ECR) assay. To 0.1 mL of fresh cell-free supernatant, 0.9 mL of ECR buffer (5 mg/mL ECR and 1 mM $CaCl_2$ in 100 mM Tris, pH 7.5) was added and incubated for 3 h at 37 °C with intermittent shaking. The reaction was terminated by adding 1 mL of sodium phosphate buffer (pH 6.0) and quickly placing the samples at 4 °C for 30 min. The insoluble ECR was separated by centrifugation and discarded. The absorbance of the supernatant was recorded at 495 nm using a UV-2600 spectrophotometer.[79]

The swimming motility of *P. aeruginosa* PAO1 was determined on soft agar plates (0.3% agar) of LB medium. Culture (5 μL) from the actively growing state (OD 600 = 0.1) was placed onto soft agar plates containing varying concentrations (25−200 μg/mL) of AuNPs-CA. No treatment was given to control plates. The plates were incubated at 37 °C for 18 h under the static condition. The swimming diameter was measured in millimeters (mm) using a transparent ruler.

Assessment of Virulence Factors of *S. marcescens* MTCC 97. For the assessment of virulence factors of *S. marcescens* MTCC 97, the culture was grown in the absence and presence of varying concentrations (25−200 μg/mL) of AuNPs-CA. The culture was grown in Luria−Bertani broth and incubated at 30 °C for 18 h in a shaking incubator. The cell-free supernatant was obtained by centrifugation at 8000 rpm for 10 min. The virulence factors of *S. marcescens* MTCC 97 were evaluated in the fresh cell-free supernatant (unless otherwise stated).

The exoprotease activity was determined using a standard azocasein degradation assay as mentioned above. Briefly, 0.1 mL of the culture supernatant was mixed with 1 mL of 0.3% (w/v) azocasein (0.5 mM $CaCl_2$ in 50 mM Tris-HCl, pH 7.5). The reaction was allowed to stand for 15 min at 30 °C with intermittent shaking. Then, 0.5 mL of ice-cold acetic acid (10%) was added to terminate the reaction. The insoluble azocasein was removed by centrifugation, and the absorbance of the supernatant was recorded at 400 nm using a UV-2600 spectrophotometer. As a blank, 50 mM Tris-HCl was used.[51]

For the determination of the prodigiosin pigment, *S. marcescens* MTCC 97 was cultured in the absence and presence of AuNPs-CA. The culture was incubated at 30 °C for 18 h under shaking. Briefly, 2 mL of culture was mixed in 1 mL of acidified ethanol (96 mL of ethanol + 4 mL of 1 M HCl) by vigorous vortexing for 5 min. The sample was centrifuged to settle down the debris and bacterial cells. The absorbance of the supernatant was recorded at 534 nm using a UV-2600 spectrophotometer. Acidified ethanol was used as a blank, and percent inhibition was calculated with respect to the control.[80]

Cell surface hydrophobicity (CSH) was determined using standard microbial adhesion to the hydrocarbon assay.[81] Bacteria were cultured in the absence and presence of varying concentrations of AuNPs-CA at 30 °C for 18 h. Following incubation, 0.1 mL of toluene was added to each treatment group and vortexed vigorously for 2 min. For the separation of two different phases, samples were incubated at room temperature for 20 min. The absorbance of the aqueous phase was recorded spectrophotometrically at 600 nm. Percent CSH was calculated using eq 3

$$\%\ \mathrm{CSH} = \left[1 - \frac{\mathrm{OD\ after\ vortexing}}{\mathrm{OD\ before\ vortexing}}\right] \times 100 \quad (3)$$

The swarming motility of *S. marcescens* MTCC 97 was examined on soft agar plates containing 0.5% agar. The soft agar plates were prepared with varying concentrations of AuNPs-CA. No amendment was done on control plates. Briefly, 5 μL of culture from the actively growing state was placed onto soft agar plates. The culture spot was allowed to air-dry in a biosafety laminar flow. The plates were incubated at 30 °C for 24 h in a static bacteriological incubator. The swarming diameter was measured using a transparent ruler in millimeters (mm).

Determination of Inhibition of Biofilm Inhibition by AuNPs-CA. The effect of AuNPs-CA on biofilms of test bacteria was assessed both spectroscopically and microscopically.

Quantitative Determination of Biofilms by the Crystal Violet Method. The quantification of biofilm inhibition by AuNPs-CA was performed using a crystal violet assay in 96-well polystyrene plates using a standard method with slight modifications.[82] The test bacteria were grown in the presence of varying concentrations (25−200 μg/mL) of AuNPs-CA in a 96-well plate for 24 h at their respective optimum temperatures in the static condition. No treatment was given in the control group. On completion of the incubation period, the medium was decanted to remove the planktonic cells. The wells containing biofilms were washed gently three times with sterile phosphate buffer to remove loosely bound cells. The biofilms were then stained by adding 200 μL of 0.1% (w/v) crystal violet solution to each well and left for 15 min. The excess amount of stain was removed, and wells were again washed thrice with sterile phosphate buffer and left at room temperature for 15 min to air-dry. Finally, the biofilms were dissolved in 250 μL of 90% ethanol and absorbance was recorded at 620 nm using a microplate reader. The percent inhibition was calculated with respect to the control.

Inhibition of Biofilms on Glass Surface. The visual validation of biofilm inhibition was performed by developing the biofilms on glass coverslips and visualizing using light, electron, and confocal microscopy.

Light Microscopy. The bacterial strains were grown in 24-well tissue culture plates in the absence and presence of 200 μg/mL AuNPs-CA. Sterile glass coverslips of dimension 1 cm

https://doi.org/10.1021/acsomega.1c02297
ACS Omega 2021, 6, 16670−16682

× 1 cm were placed in each well in the slant position and incubated for 24 h at their respective optimum temperatures under the static condition. Following incubation, the glass coverslips were removed and gently washed with sterile phosphate buffer to wash out loosely bound cells. The biofilms on the glass surface were stained for 15 min by placing a few drops of 0.1% (w/v) crystal violet solution. The excess stain was washed with sterile phosphate buffer and left at room temperature to air-dry. The biofilms were visualized using a light microscope (Olympus BX60, model BX60F5, Olympus Optical Co. Ltd. Japan) equipped with a color VGA camera (Sony, model no. SSC−DC-58AP, Japan), and images were captured at 40X magnification.

Confocal Microscopy. For confocal microscopy, the biofilms were developed on a glass surface as mentioned above. The glass coverslips were taken out and washed with sterile phosphate buffer. The biofilms were stained for 20 min using 0.1% acridine orange. The excess amount of stain was removed by washing. The glass coverslips were air-dried at room temperature in the dark. The images were captured using Zeiss LSM780 at 63X magnification, at USIF, AMU, Aligarh.

Scanning Electron Microscopy. The glass coverslips containing biofilms were developed as mentioned in the Light Microscopy section. The glass coverslips were washed with sterile phosphate buffer and air-dried for 15 min at room temperature. The biofilms were fixed with 2.5% glutaraldehyde (prepared in 50 mM phosphate buffer) for 24 h at 4 °C. After fixation, the biofilms were dehydrated by a gradient of ethanol washing ranging from 20 to 100%. Each gradient wash was done for 15 min. The coverslips were air-dried at room temperature and then coated with gold. The visualization was done using a JEOL-JSM 6510 LV scanning electron microscope, at USIF, AMU, Aligarh.

Determination of Exopolysaccharides (EPS) Inhibition by AuNPs-CA. The estimation of exopolysaccharides (EPS) was done in the cell-free supernatant using a previously described method with minor modifications.[83] Briefly, test bacteria were cultured in the absence and presence of varying concentrations (25−200 μg/mL) of AuNPs-CA. The cultures were incubated for 24 h at their respective optimum growth temperatures in a shaking incubator. The cell-free supernatant was obtained by centrifugation. The EPS was precipitated by adding 15 mL of chilled ethanol to 5 mL of culture supernatant and incubated overnight at 4 °C. The amount of EPS was determined by estimating the sugar level using the Dubois method.[84]

Statistical Analysis. Each experiment was performed in three independent replicates, and data presented are average with standard deviation. For analysis of statistical significance, the two-sample *t*-test was performed.

■ ASSOCIATED CONTENT

Supporting Information

The Supporting Information is available free of charge at https://pubs.acs.org/doi/10.1021/acsomega.1c02297.

Percent inhibition of virulence factors of *P. aeruginosa* PAO1 and *S. marcescens* MTCC 97; viable counts of bacteria in the presence of AuNPs-CA (PDF)

■ AUTHOR INFORMATION

Corresponding Author

Faizan Abul Qais − *Department of Agricultural Microbiology, Faculty of Agricultural Sciences, Aligarh Muslim University, Aligarh 202002, UP, India;* orcid.org/0000-0002-9457-6515; Email: faizanabulqais@gmail.com

Authors

Iqbal Ahmad − *Department of Agricultural Microbiology, Faculty of Agricultural Sciences, Aligarh Muslim University, Aligarh 202002, UP, India;* orcid.org/0000-0001-8447-4497

Mohammad Altaf − *Department of Chemistry, College of Science and Central Laboratory, College of Science, King Saud University, Riyadh 11451, Saudi Arabia*

Saad H. Alotaibi − *Department of Chemistry, Turabah University College, Taif University, Taif 21944, Saudi Arabia*

Complete contact information is available at: https://pubs.acs.org/10.1021/acsomega.1c02297

Notes

The authors declare no competing financial interest.

■ ACKNOWLEDGMENTS

We acknowledge Taif University for Researchers Supporting Project number (TURSP-2020/83), Taif University, Taif, Saudi Arabia. FAQ is thankful to CSIR {File no. 09/112(0626) 2k19 EMR} for providing SRF.

■ ABBREVIATIONS

CSH:cell surface hydrophobicity; ECR:Elastin−Congo red; EPS:exopolysaccharides; QS:quorum sensing; SEM:scanning electron microscopy; TCA:trichloroacetic acid

■ REFERENCES

(1) WHO. *The Top 10 Causes of Death*; World Health Organization, 2018.

(2) Shakoor, S.; Platts-Mills, J. A.; Hasan, R. Antibiotic-Resistant Enteric Infections. *Infect. Dis. Clin. North Am.* **2019**, *33*, 1105−1123.

(3) Andleeb, S.; Majid, M.; Sardar, S. Environmental and Public Health Effects of Antibiotics and AMR/ARGs. In *Antibiotics and Antimicrobial Resistance Genes in the Environment*; Elsevier, 2020; pp 269−291.

(4) Dadgostar, P. Antimicrobial Resistance: Implications and Costs. *Infect. Drug Resist.* **2019**, *12*, 3903−3910.

(5) WHO. *No Time to Wait: Securing the Future from Drug-Resistant Infections*; World Health Organization, 2019.

(6) USCDC. *Antibiotic Resistance Threats in the United States*; Centers for Disease Control and Prevention, 2013; Vol. 23, pp11−28.

(7) Kalia, V. C. Quorum Sensing Inhibitors: An Overview. *Biotechnol. Adv.* **2013**, *31*, 224−245.

(8) Piewngam, P.; Chiou, J.; Chatterjee, P.; Otto, M. Alternative Approaches to Treat Bacterial Infections: Targeting Quorum-Sensing. *Expert Rev. Anti-Infect. Ther.* **2020**, *18*, 499−510.

(9) Khan, M. S.; Qais, F. A.; Ahmad, I. Quorum Sensing Interference by Natural Products from Medicinal Plants: Significance in Combating Bacterial Infection. In *Biotechnological Applications of Quorum Sensing Inhibitors*; Springer: Singapore, 2018; pp 417−445.

(10) Saeki, E. K.; Kobayashi, R. K. T.; Nakazato, G. Quorum Sensing System: Target to Control the Spread of Bacterial Infections. *Microb. Pathog.* **2020**, *142*, No. 104068.

(11) Rutherford, S. T.; Bassler, B. L. Bacterial Quorum Sensing: Its Role in Virulence and Possibilities for Its Control. *Cold Spring Harbor Perspect. Biol.* **2012**, *2*, No. a012427.

(12) Hernando-Amado, S.; Sanz-García, F.; Martínez, J. L. Antibiotic Resistance Evolution Is Contingent on the Quorum-Sensing Response in *Pseudomonas aeruginosa*. *Mol. Biol. Evol.* **2019**, *36*, 2238−2251.
(13) Lopez, D.; Vlamakis, H.; Kolter, R. Biofilms. *Cold Spring Harbor Perspect. Biol.* **2010**, *2*, No. a000398.
(14) Karygianni, L.; Ren, Z.; Koo, H.; Thurnheer, T. Biofilm Matrixome: Extracellular Components in Structured Microbial Communities. *Trends Microbiol.* **2020**, *28*, 668−681.
(15) Rau, J. V.; De Santis, R.; Ciofani, G. Exploring Challenges Ahead of Nanotechnology for Biomedicine. *Bioact. Mater.* **2017**, *2*, 119−120.
(16) Bhardwaj, V.; Kaushik, A. Biomedical Applications of Nanotechnology and Nanomaterials. *Micromachines* **2017**, *8*, No. 298.
(17) Hajipour, M. J.; Fromm, K. M.; Akbar Ashkarran, A.; Jimenez de Aberasturi, D.; Larramendi, I. R. de.; Rojo, T.; Serpooshan, V.; Parak, W. J.; Mahmoudi, M. Antibacterial Properties of Nanoparticles. *Trends Biotechnol.* **2012**, *30*, 499−511.
(18) Chaudhary, S.; Jyoti, A.; Shrivastava, V.; Tomar, R. S. Role of Nanoparticles as Antibiofilm Agents: A Comprehensive Review. *Curr. Trends Biotechnol. Pharm.* **2020**, *14*, 97−110.
(19) Tagad, C. K.; Dugasani, S. R.; Aiyer, R.; Park, S.; Kulkarni, A.; Sabharwal, S. Green Synthesis of Silver Nanoparticles and Their Application for the Development of Optical Fiber Based Hydrogen Peroxide Sensor. *Sens. Actuators, B* **2013**, *183*, 144−149.
(20) Abdel-Halim, E. S.; El-Rafie, M. H.; Al-Deyab, S. S. Polyacrylamide/Guar Gum Graft Copolymer for Preparation of Silver Nanoparticles. *Carbohydr. Polym.* **2011**, *85*, 692−697.
(21) Zubair, M.; Husain, F. M.; Qais, F. A.; Alam, P.; Ahmad, I.; Albalawi, T.; Ahmad, N.; Alam, M.; Baig, M. H.; Dong, J.-J.; Fatima, F.; Alsayed, B. Bio-Fabrication of Titanium Oxide Nanoparticles from Ochradenus Arabicus to Obliterate Biofilms of Drug-Resistant *Staphylococcus aureus* and *Pseudomonas aeruginosa* Isolated from Diabetic Foot Infections. *Appl. Nanosci.* **2021**, *11*, 375−387.
(22) Shayan, S.; Saeidi, S. Antibacterial and Antibiofilm Activities of Extract *Capsicum annuum* L on the Growth and Biofilm Formation of Common Pathogenic Strains. *Int. Res. J. Appl. Basic Sci.* **2013**, *5*, 513−518.
(23) Rivera, M. L. C.; Hassimotto, N. M. A.; Bueris, V.; Sircili, M. P.; Almeida, F. A.; Pinto, U. M. Effect of *Capsicum frutescens* Extract, Capsaicin, and Luteolin on Quorum Sensing Regulated Phenotypes. *J. Food Sci.* **2019**, *84*, 1477−1486.
(24) Samanta, S.; Singh, B. R.; Adholeya, A. Intracellular Synthesis of Gold Nanoparticles Using an Ectomycorrhizal Strain EM-1083 of Laccaria Fraterna and Its Nanoanti-Quorum Sensing Potential Against *Pseudomonas aeruginosa*. *Indian J. Microbiol.* **2017**, *57*, 448−460.
(25) Dharul Salam, F.; Nadar Vinita, M.; Puja, P.; Prakash, S.; Yuvakkumar, R.; Kumar, P. Anti-Bacterial and Anti-Biofilm Efficacies of Bioinspired Gold Nanoparticles. *Mater. Lett.* **2020**, *261*, No. 126998.
(26) Yuan, C.-G.; Huo, C.; Yu, S.; Gui, B. Biosynthesis of Gold Nanoparticles Using *Capsicum annuum* Var. Grossum Pulp Extract and Its Catalytic Activity. *Phys. E* **2017**, *85*, 19−26.
(27) Dey, A.; Yogamoorthy, A.; Sundarapandian, S. Green Synthesis of Gold Nanoparticles and Evaluation of Its Cytotoxic Property against Colon Cancer Cell Line. *Res. J. Life Sci., Bioinf., Pharm. Chem. Sci.* **2018**, *4*, 1−17.
(28) Liu, X.; Atwater, M.; Wang, J.; Huo, Q. Extinction Coefficient of Gold Nanoparticles with Different Sizes and Different Capping Ligands. *Colloids Surf., B* **2007**, *58*, 3−7.
(29) Pop, O. L.; Mesaros, A.; Vodnar, D. C.; Suharoschi, R.; Tăbăran, F.; Mageruşan, L.; Tódor, I. S.; Diaconeasa, Z.; Balint, A.; Ciontea, L.; Socaciu, C. Cerium Oxide Nanoparticles and Their Efficient Antibacterial Application In Vitro against Gram-Positive and Gram-Negative Pathogens. *Nanomaterials* **2020**, *10*, No. 1614.
(30) Dietrich, L. E. P.; Price-Whelan, A.; Petersen, A.; Whiteley, M.; Newman, D. K. The Phenazine Pyocyanin Is a Terminal Signalling Factor in the Quorum Sensing Network of *Pseudomonas aeruginosa*. *Mol. Microbiol.* **2006**, *61*, 1308−1321.
(31) Lau, G. W.; Hassett, D. J.; Ran, H.; Kong, F. The Role of Pyocyanin in *Pseudomonas aeruginosa* Infection. *Trends Mol. Med.* **2004**, *10*, 599−606.
(32) Fothergill, J. L.; Panagea, S.; Hart, C. A.; Walshaw, M. J.; Pitt, T. L.; Winstanley, C. Widespread Pyocyanin Over-Production among Isolates of a Cystic Fibrosis Epidemic Strain. *BMC Microbiol.* **2007**, *7*, No. 45.
(33) Das, T.; Kutty, S. K.; Tavallaie, R.; Ibugo, A. I.; Panchompoo, J.; Sehar, S.; Aldous, L.; Yeung, A. W. S.; Thomas, S. R.; Kumar, N.; Gooding, J. J.; Manefield, M. Phenazine Virulence Factor Binding to Extracellular DNA Is Important for *Pseudomonas aeruginosa* Biofilm Formation. *Sci. Rep.* **2015**, *5*, No. 8398.
(34) Peek, M. E.; Bhatnagar, A.; McCarty, N. A.; Zughaier, S. M. Pyoverdine, the Major Siderophore in *Pseudomonas aeruginosa*, Evades NGAL Recognition. *Interdiscip. Perspect. Infect. Dis.* **2012**, *2012*, No. 843509.
(35) Cox, C.; Adams, P. Siderophore Activity of Pyoverdin for *Pseudomonas aeruginosa*. *Infect. Immun.* **1985**, *48*, 130−138.
(36) Bejarano, P. A.; Langeveld, J. P.; Hudson, B. G.; Noelken, M. E. Degradation of Basement Membranes by *Pseudomonas aeruginosa* Elastase. *Infect. Immun.* **1989**, *57*, 3783−3787.
(37) Smith, R. S.; Iglewski, B. H.; Barbara, H. *P. aeruginosa* Quorum-Sensing Systems and Virulence. *Curr. Opin. Microbiol.* **2003**, *6*, 56−60.
(38) Yu, H.; He, X.; Xie, W.; Xiong, J.; Sheng, H.; Guo, S.; Huang, C.; Zhang, D.; Zhang, K. Elastase LasB of *Pseudomonas aeruginosa* Promotes Biofilm Formation Partly through Rhamnolipid-Mediated Regulation. *Can. J. Microbiol.* **2014**, *60*, 227−235.
(39) Khan, F.; Manivasagan, P.; Lee, J.-W.; Pham, D.; Oh, J.; Kim, Y.-M. Fucoidan-Stabilized Gold Nanoparticle-Mediated Biofilm Inhibition, Attenuation of Virulence and Motility Properties in *Pseudomonas aeruginosa* PAO1. *Mar. Drugs* **2019**, *17*, No. 208.
(40) Singh, B. R.; Singh, B. N.; Singh, A.; Khan, W.; Naqvi, A. H.; Singh, H. B. Mycofabricated Biosilver Nanoparticles Interrupt *Pseudomonas aeruginosa* Quorum Sensing Systems. *Sci. Rep.* **2015**, *5*, No. 13719.
(41) Davey, M. E.; Caiazza, N. C.; O'Toole, G. A. Rhamnolipid Surfactant Production Affects Biofilm Architecture in *Pseudomonas aeruginosa* PAO1. *J. Bacteriol.* **2003**, *185*, 1027−1036.
(42) Köhler, T.; Curty, L. K.; Barja, F.; van Delden, C.; Pechère, J. C. Swarming of *Pseudomonas aeruginosa* Is Dependent on Cell-to-Cell Signaling and Requires Flagella and Pili. *J. Bacteriol.* **2000**, *182*, 5990−5996.
(43) Beatson, S. A.; Whitchurch, C. B.; Semmler, A. B. T.; Mattick, J. S. Quorum Sensing Is Not Required for Twitching Motility in *Pseudomonas aeruginosa*. *J. Bacteriol.* **2002**, *184*, 3598−3604.
(44) Lahiri, D.; Nag, M.; Sheikh, H. I.; Sarkar, T.; Edinur, H. A.; Pati, S.; Ray, R. R. Microbiologically-Synthesized Nanoparticles and Their Role in Silencing the Biofilm Signaling Cascade. *Front. Microbiol.* **2021**, *12*, No. 636588.
(45) Singh, R.; Shedbalkar, U. U.; Wadhwani, S. A.; Chopade, B. A. Bacteriagenic Silver Nanoparticles: Synthesis, Mechanism, and Applications. *Appl. Microbiol. Biotechnol.* **2015**, *99*, 4579−4593.
(46) Wei, J.-R.; Lai, H.-C. N-Acylhomoserine Lactone-Dependent Cell-to-Cell Communication and Social Behavior in the Genus Serratia. *Int. J. Med. Microbiol.* **2006**, *296*, 117−124.
(47) Goluszko, P.; Nowicki, B.; Goluszko, E.; Nowicki, S.; Kaul, A.; Pham, T. Association of Colony Variation in *Serratia marcescens* with the Differential Expression of Protease and Type 1 Fimbriae. *FEMS Microbiol. Lett.* **1995**, *133*, 41−45.
(48) Liu, G. Y.; Nizet, V. Color Me Bad: Microbial Pigments as Virulence Factors. *Trends Microbiol.* **2009**, *17*, 406−413.
(49) Srinivasan, R.; Vigneshwari, L.; Rajavel, T.; Durgadevi, R.; Kannappan, A.; Balamurugan, K.; Pandima Devi, K.; Veera Ravi, A. Biogenic Synthesis of Silver Nanoparticles Using *Piper betle* Aqueous Extract and Evaluation of Its Anti-Quorum Sensing and Antibiofilm Potential against Uropathogens with Cytotoxic Effects: An in Vitro

https://doi.org/10.1021/acsomega.1c02297
ACS Omega 2021, 6, 16670−16682

and in Vivo Approach. *Environ. Sci. Pollut. Res.* **2018**, *25*, 10538−10554.
(50) Kida, Y.; Inoue, H.; Shimizu, T.; Kuwano, K. *Serratia marcescens* Serralysin Induces Inflammatory Responses through Protease-Activated Receptor 2. *Infect. Immun.* **2007**, *75*, 164−174.
(51) Salini, R.; Pandian, S. K. Interference of Quorum Sensing in Urinary Pathogen *Serratia marcescens* by Anethum Graveolens. *Pathog. Dis.* **2015**, *73*, No. ftv038.
(52) Ravindran, D.; Ramanathan, S.; Arunachalam, K.; Jeyaraj, G. P.; Shunmugiah, K. P.; Arumugam, V. R. Phytosynthesized Silver Nanoparticles as Antiquorum Sensing and Antibiofilm Agent against the Nosocomial Pathogen *Serratia marcescens*: An in Vitro Study. *J. Appl. Microbiol.* **2018**, *124*, 1425−1440.
(53) Srinivasan, R.; Devi, K. R.; Kannappan, A.; Pandian, S. K.; Ravi, A. V. *Piper betle* and Its Bioactive Metabolite Phytol Mitigates Quorum Sensing Mediated Virulence Factors and Biofilm of Nosocomial Pathogen *Serratia marcescens* in Vitro. *J. Ethnopharmacol.* **2016**, *193*, 592−603.
(54) Balashanmugam, P.; Durai, P.; Balakumaran, M. D.; Kalaichelvan, P. T. Phytosynthesized Gold Nanoparticles from C. roxburghii DC. Leaf and Their Toxic Effects on Normal and Cancer Cell Lines. *J. Photochem. Photobiol., B* **2016**, *165*, 163−173.
(55) Ramalingam, V.; Revathidevi, S.; Shanmuganayagam, T.; Muthulakshmi, L.; Rajaram, R. Biogenic Gold Nanoparticles Induce Cell Cycle Arrest through Oxidative Stress and Sensitize Mitochondrial Membranes in A549 Lung Cancer Cells. *RSC Adv.* **2016**, *6*, 20598−20608.
(56) Sun, H.; Jia, J.; Jiang, C.; Zhai, S. Gold Nanoparticle-Induced Cell Death and Potential Applications in Nanomedicine. *Int. J. Mol. Sci.* **2018**, *19*, No. 754.
(57) Burmølle, M.; Thomsen, T. R.; Fazli, M.; Dige, I.; Christensen, L.; Homøe, P.; Tvede, M.; Nyvad, B.; Tolker-Nielsen, T.; Givskov, M.; Moser, C.; Kirketerp-Møller, K.; Johansen, H. K.; Høiby, N.; Jensen, P. Ø.; Sørensen, S. J.; Bjarnsholt, T. Biofilms in Chronic Infections—a Matter of Opportunity—Monospecies Biofilms in Multispecies Infections. *FEMS Immunol. Med. Microbiol.* **2010**, *59*, 324−336.
(58) Hooper, S. J.; Percival, S. L.; Cochrane, C. A.; Williams, D. W. Biofilms and Implication in Medical Devices in Humans and Animals. In *Biofilms and Veterinary Medicine*; Springer: Berlin, Heidelberg, 2011; pp 191−203.
(59) Percival, S. L.; Hill, K. E.; Williams, D. W.; Hooper, S. J.; Thomas, D. W.; Costerton, J. W. A Review of the Scientific Evidence for Biofilms in Wounds. *Wound Repair Regener.* **2012**, *20*, 647−657.
(60) Woods, E. J.; Davis, P.; Barnett, J. P. S. Wound Healing Immunology and Biofilms. In *Microbiology of Wounds*; CRC Press: London, 2010; pp 271−92.
(61) Parsek, M. R.; Singh, P. K. Bacterial Biofilms: An Emerging Link to Disease Pathogenesis. *Annu. Rev. Microbiol.* **2003**, *57*, 677−701.
(62) Nickel, J. C.; Ruseska, I.; Wright, J. B.; Costerton, J. W. Tobramycin Resistance of *Pseudomonas aeruginosa* Cells Growing as a Biofilm on Urinary Catheter Material. *Antimicrob. Agents Chemother.* **1985**, *27*, 619−624.
(63) Deshpande, S.; Patil, S.; Kuchibhatla, S. V.; Seal, S. Size Dependency Variation in Lattice Parameter and Valency States in Nanocrystalline Cerium Oxide. *Appl. Phys. Lett.* **2005**, *87*, No. 133113.
(64) Rispoli, F.; Angelov, A.; Badia, D.; Kumar, A.; Seal, S.; Shah, V. Understanding the Toxicity of Aggregated Zero Valent Copper Nanoparticles against *Escherichia coli*. *J. Hazard. Mater.* **2010**, *180*, 212−216.
(65) Sahle-Demessie, E.; Tadesse, H. Kinetics and Equilibrium Adsorption of Nano-TiO2 Particles on Synthetic Biofilm. *Surf. Sci.* **2011**, *605*, 1177−1184.
(66) Shkodenko, L.; Kassirov, I.; Koshel, E. Metal Oxide Nanoparticles Against Bacterial Biofilms: Perspectives and Limitations. *Microorganisms* **2020**, *8*, No. 1545.
(67) Majumdar, M.; Biswas, S. C.; Choudhury, R.; Upadhyay, P.; Adhikary, A.; Roy, D. N.; Misra, T. K. Synthesis of Gold Nanoparticles Using Citrus Macroptera Fruit Extract: Anti-Biofilm and Anticancer Activity. *ChemistrySelect* **2019**, *4*, 5714−5723.
(68) Decho, A. W.; Gutierrez, T. Microbial Extracellular Polymeric Substances (EPSs) in Ocean Systems. *Front. Microbiol.* **2017**, *8*, No. 922.
(69) Sauer, K.; Camper, A. K. Characterization of Phenotypic Changes In Pseudomonas Putida in Response to Surface-Associated Growth. *J. Bacteriol.* **2001**, *183*, 6579−6589.
(70) Fux, C. A.; Costerton, J. W.; Stewart, P. S.; Stoodley, P. Survival Strategies of Infectious Biofilms. *Trends Microbiol.* **2005**, *13*, 34−40.
(71) Yildiz, F. H.; Schoolnik, G. K. Vibrio Cholerae O1 El Tor: Identification of a Gene Cluster Required for the Rugose Colony Type, Exopolysaccharide Production, Chlorine Resistance, and Biofilm Formation. *Proc. Natl. Acad. Sci. U.S.A.* **1999**, *96*, 4028−4033.
(72) Czaczyk, K.; Myszka, K. Biosynthesis of Extracellular Polymeric Substances (EPS) and Its Role in Microbial Biofilm Formation. *Pol. J. Environ. Stud.* **2007**, *16*, 799−806.
(73) Rajkumari, J.; Busi, S.; Vasu, A. C.; Reddy, P. Facile Green Synthesis of Baicalein Fabricated Gold Nanoparticles and Their Antibiofilm Activity against *Pseudomonas aeruginosa* PAO1. *Microb. Pathog.* **2017**, *107*, 261−269.
(74) Jayaseelan, C.; Ramkumar, R.; Rahuman, A. A.; Perumal, P. Green Synthesis of Gold Nanoparticles Using Seed Aqueous Extract of Abelmoschus Esculentus and Its Antifungal Activity. *Ind. Crops Prod.* **2013**, *45*, 423−429.
(75) Peter, J.; Backialakshmi, M.; Karpagavinayagam, P.; Vedhi, C. Green Synthesis and Characterization of Colloidal Gold Nanoparticles for Optical Properties. *J. Adv. Chem. Sci.* **2014**, *1*, 1−5.
(76) Essar, D. W.; Eberly, L.; Hadero, A.; Crawford, I. P. Identification and Characterization of Genes for a Second Anthranilate Synthase in *Pseudomonas aeruginosa*: Interchangeability of the Two Anthranilate Synthase and Evolutionary Implications. *J. Bacteriol.* **1990**, *172*, 884−900.
(77) Ankenbauer, R.; Sriyosachati, S.; Cox, C. D. Effects of Siderophores on the Growth of *Pseudomonas aeruginosa* in Human Serum and Transferrin. *Infect. Immun.* **1985**, *49*, 132−140.
(78) Husain, F. M.; Ahmad, I.; Al-Thubiani, A. S.; Abulreesh, H.; AlHazza, I. M.; Aqil, F. Leaf Extracts of Mangifera Indica L. Inhibit Quorum Sensing—Regulated Production of Virulence Factors and Biofilm in Test Bacteria. *Front. Microbiol.* **2017**, *8*, No. 727.
(79) Kessler, E.; Israel, M.; Landshman, N.; Chechick, A.; Blumberg, S. In Vitro Inhibition of *Pseudomonas aeruginosa* Elastase by Metal-Chelating Peptide Derivatives. *Infect. Immun.* **1982**, *38*, 716−723.
(80) Slater, H.; Crow, M.; Everson, L.; Salmond, G. P. C. Phosphate Availability Regulates Biosynthesis of Two Antibiotics, Prodigiosin and Carbapenem, in Serratia via Both Quorum-Sensing-Dependent and -Independent Pathways. *Mol. Microbiol.* **2003**, *47*, 303−320.
(81) Courtney, H. S.; Ofek, I.; Penfound, T.; Nizet, V.; Pence, M. A.; Kreikemeyer, B.; Podbielbski, A.; Hasty, D. L.; Dale, J. B. Relationship between Expression of the Family of M Proteins and Lipoteichoic Acid to Hydrophobicity and Biofilm Formation in Streptococcus Pyogenes. *PLoS One* **2009**, *4*, No. e4166.
(82) O'Toole, G. A.; Kolter, R. Flagellar and Twitching Motility Are Necessary for *Pseudomonas aeruginosa* Biofilm Development. *Mol. Microbiol.* **1998**, *30*, 295−304.
(83) Hasan, I.; Qais, F. A. F. A.; Husain, F. M. F. M.; Khan, R. A. R. A.; Alsalme, A.; Alenazi, B.; Usman, M.; Jaafar, M. H.; Ahmad, I. Eco-Friendly Green Synthesis of Dextrin Based Poly (Methyl Methacrylate) Grafted Silver Nanocomposites and Their Antibacterial and Antibiofilm Efficacy against Multi-Drug Resistance Pathogens. *J. Cleaner Prod.* **2019**, *230*, 1148−1155.
(84) DuBois, M.; Gilles, K. A.; Hamilton, J. K.; Rebers, P. A.; Smith, F. Colorimetric Method for Determination of Sugars and Related Substances. *Anal. Chem.* **1956**, *28*, 350−356.

https://doi.org/10.1021/acsomega.1c02297
ACS Omega 2021, 6, 16670−16682